DRAFT Proceedings of the ASME2016 International Mechanical Engineering Congress and Exposition (IMECE)
November 11 - 17, 2016, Phoenix, Arizona, USA

IMECE2016-66523

USING AN EXTENDABLE BUMPER WITH AN AID OF VEHICLE DYNAMICS CONTROL SYSTEM TO IMPROVE THE OCCUPANT SAFETY IN FRONTAL VEHICLE-TO-VEHICLE COLLISION SCENARIO

Mustafa Elkady
Lebanese International University
Beirut, Lebanon

Ahmed Elmarakbi
University of Sunderland
Sunderland SR60DD, UK

John MacIntyre
University of Sunderland
Sunderland SR60DD, UK

ABSTRACT

This paper aims to improve vehicle crashworthiness using vehicle dynamics control systems (VDCS) integrated with an extendable front-end structure (extendable bumper). The work carried out in this paper includes developing and analyzing a new vehicle dynamics/crash mathematical model and a multi-body occupant mathematical model in case of vehicle-to-vehicle full frontal impact. The first model integrates a vehicle dynamics model with the vehicle's front-end structure to define the vehicle body crash kinematic parameters. In this model, the anti-lock braking system (ABS) and the active suspension control system (ASC) are co-simulated, and its associated equations of motion are developed and solved numerically. The second model is used to capture the occupant kinematics during full frontal collision. The simulations show considerable improvements using VDCS with and without the extendable bumper (EB), which produces additional significant improvements for both vehicle boy acceleration and intrusion.

INTRODUCTION

The increasing public awareness of safety issues and the increasing legislative requirements have increased the pressure on vehicle manufacturers to improve the vehicle crashworthiness. Accident analyses have shown that two-thirds of the collisions in which car occupants have been injured are frontal collisions (1, 2). Despite worldwide advances in research programs to develop intelligent safety systems, frontal collision remains to be the major source of road fatalities and serious injuries for decades to come (3). The evaluation of the deformation behavior of the front-end of passenger vehicles has been based on the assumption that in frontal collisions, the kinetic energy of the vehicle should be transformed into plastic deformation with a minimum deformation of the vehicle (4).

Many different techniques were studied to investigate the opportunities of the vehicle collision mitigation. These techniques can be classified as pre and post-collision. The most well-known pre-collision method is the advance driver assistant systems (ADAS). The aim of ADAS is to mitigate and avoid vehicle frontal collisions. The main idea of ADAS is to collect data from the road (i.e. traffic lights, other cars distances and velocities, obstacles etc.) and transfer this information to the driver, warn the driver in danger situations and aide the driver actively in imminent collision.

There are different actions may be taken when these systems detect that the collision is unavoidable. For example, the brake assistant system (BAS) (5) and the collision mitigation brake system (CMBS) (6) were used to activate the braking instantly based on the behavior characteristics of the driver, and relative position from the most dangerous other object for the moment. While ADAS was investigated, developed, and already used for some modern vehicles, it is still far away from its goal to prevent vehicle collisions.

In terms of the enhancing crash energy absorption and minimizing deformation of the vehicle's structure in post-collision, two types of smart front-end structures, namely: extendable and fixed, have been proposed and analyzed to mitigate vehicle collision and enhance crash behavior in different crash scenarios (7, 8). The extendable smart front-end

structure, which is considered in this paper, consists of two hydraulic cylinders integrated with the front-end longitudinal members of standard vehicles. The hydraulic cylinders can be extended in impending collisions using radar techniques to absorb the impact kinetic energy proving that smart structure can absorb more crash energy by their damping characteristics. For this smart structure, several mathematical models were developed and analytical and numerical simulations were presented (7, 8).

Modern motor vehicles are increasingly using vehicle dynamic control systems (VDCS) to replace traditional mechanical systems in order to improve vehicle handling, stability, and comfort. In addition, VDCS are playing an important role for active safety system for road vehicles, which control the dynamic vehicle motion in emergency situations. Anti-lock brake system (ABS) is used to allow the vehicle to follow the desired steering angle while the intense braking is applied (9). In addition, the ABS helps reducing the stopping distance of a vehicle compared with the conventional braking system. The Active suspension control system (ASC) is used to improve the quality of the vehicle ride and reduce the vertical acceleration (10, 11).

An extensive review of the current literatures showed that a little research exists on the influences of vehicle dynamics on vehicle collisions. The influence of the braking force on vehicle impact dynamics in low-speed rear-end collisions has been studied (12). It was confirmed that the braking force was not negligible in high-quality simulations of vehicle impact dynamics at low speed. The effect of vehicle braking on the crash and the possibility of using vehicle dynamics control systems to reduce the risk of incompatibility and improve the crash performance in frontal vehicle-to-barrier collision were investigated (13). They proved that there is a slight improvement of the vehicle deformation once the brakes are applied during the crash. A multibody vehicle dynamic model using ADAMS software, alongside with a simple crash model was generated in order to study the effects of the implemented control strategy.

In this paper a unique vehicle crash/dynamics mathematical model and a multi-body occupant mathematical model are developed. These models are used to investigate the mitigation of the vehicle collision in the case of full frontal vehicle-to-vehicle crash scenario using VDCS and an extendable bumper.

MATHEMATICAL MODELLING

Vehicle dynamics/crash model - The main advantage of the mathematical modelling (using numerical and/or analytical solutions) is producing a reliable quick simulation results. The mathematical modelling tool is preferable in the first stage of design to avoid the high computational costs using Finite Element (FE) models. Two analytical models were created using a computer simulation, one for vehicle component crash and the other for barrier impact statically and then both models were merged into one model (14). To achieve enhanced occupant safety, the crash energy management system was explored (15). In his study, he used a simple lumped-parameter model and discussed the applicability of providing variable energy-absorbing properties as a function of the impact speed.

In this paper, 8-Degree- of- Freedom (DoF) vehicle dynamics/ crash mathematical models is developed to study the effect of vehicle dynamics control systems on vehicle collision mitigation. Full frontal vehicle-to-vehicle crash scenario is considered in this study.

As shown in Figure 1, vehicle "**a**" represents the vehicle equipped with extendable front-end structure and vehicle "**b**" represents the existing standard vehicle. The impact initial velocities of both vehicle "**a**" and vehicle "**b**" are v_a and v_b, respectively.

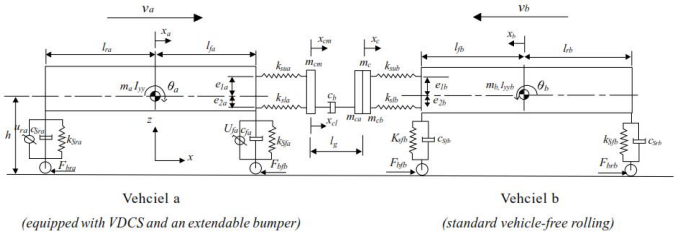

FIGURE 1. VEHICLE-TO-VEHICLE FULL FRONTAL COLLISION

In this model, the vehicle body is represented by lumped mass m and it has a translational motion on longitudinal direction (x-axis), translational motion on vertical direction (z-axis) and pitching motion (around y-axis). The front-end structure is represented by two non-linear springs with stiffness's k_{su} and k_{sl} for the upper members (rails) and the lower members of the vehicle frontal structure, respectively. The hydraulic cylinders, with length l_g, are represented by dampers of vehicle "**b**" is represented by m_{cb}. It is worthwhile noting that in the case of vehicle-to-vehicle frontal collision, the masses of the two bumpers (bumpers assembly), m_{ca} and m_{cb}, are assumed to be in contact throughout the crash process and have the same velocity and displacement in longitudinal x direction. The mass of the two bumpers are defined by m_c and provides a mechanism of load transfer from one longitudinal to the other.

The ABS and the ASC systems are co-simulated with a vehicle dynamic model and integrated with a non-linear front-end structure model combined with an extendable bumper as shown in Figure 1. The general dimensions of the model are shown in Figure 1, where l_f, l_r, h, e_1 and e_2 represent the longitudinal distance between the vehicle's centre of gravity (CG) and front wheels, the longitudinal distance between the CG and rear wheels, the high of the CG from the ground, the distance between the CG and front-end upper springs and the CG and front- end lower springs respectively. At the first stage of impact, deformation of the front-end and vehicle pitching are small and only the lower members are deformed through the extendable bumper. At the end of impact the deformation of the front-end reaches its maximum level (for the upper and lower members), vehicle pitch angle increases and the rear wheels leave the ground. It is assumed that the front-end

springs are still horizontal during impact, and they will not incline with the vehicle body.

Two spring/damper units are used to represent the conventional vehicle suspension systems. Each unit has a spring stiffness k_S and a damping coefficient c. The subscripts f and r, u and l denote the front and rear wheels, upper and lower longitudinal members, respectively. The ASC system is co-simulated with the conventional suspension system to add or subtract an active force element u. The AB is co-simulated with the mathematical model using a simple wheel model. The unsprung masses are not considered in this model and it is assumed that the vehicle moves on a flat-asphalted road, which means that the vertical movement of the tyres and road vertical forces can be neglected.

The equations of motion of the mathematical model are developed to study and predict the dynamic response of the vehicle-to-vehicle in full frontal crash scenario as follows:

$$m_a \cdot \ddot{x}_a + F_{sua} + F_{sla} + F_{bfa} + F_{bra} = 0 \quad (1)$$

$$m_b \cdot \ddot{x}_b + F_{sub} + F_{slb} + F_{bfb} + F_{brb} = 0 \quad (2)$$

$$m_a \cdot \ddot{z}_a + F_{Sfa} + F_{Sra} = 0 \quad (3)$$

$$m_b \cdot \ddot{z}_b + F_{Sfb} + F_{Srb} = 0 \quad (4)$$

$$I_{yya} \cdot \ddot{\theta}_a - F_{Sfa} \cdot l_{fa} + F_{Sra} \cdot l_{ra} + F_{sua} \cdot d_{1a} - F_{sla} \cdot d_{2a} - (F_{bfa} + F_{bra}) \cdot (z_a + h_a) = 0 \quad (5)$$

$$I_{yyb} \cdot \ddot{\theta}_b - F_{Sfb} \cdot l_{fb} + F_{Srb} \cdot l_{rb} + F_{sub} \cdot d_{1b} - F_{slb} \cdot d_{2b} - (F_{bfb} + F_{brb}) \cdot (z_b + h_b) = 0 \quad (6)$$

$$m_{cm} \cdot \ddot{x}_{cm} + F_d - F_{sua} - F_{sla} = 0 \quad (7)$$

$$m_c \cdot \ddot{x}_c - F_d + F_{sub} + F_{slb} = 0 \quad (8)$$

The scripts $\ddot{x}$ and $\ddot{z}$ are the acceleration of the vehicle body in longitudinal direction and vertical directions, respectively. $\ddot{\theta}$ is the rotational pitching acceleration of the vehicle body. Subscripts a, b, c_m and c represents vehicle "**a**", vehicle "**b**", cross member of vehicle "**a**" and the two vehicle bumpers, respectively. F_s, F_S, F_b and F_d are front-end non-linear spring forces, vehicle suspension forces, braking forces and the damping force of the extendable bumper hydraulic cylinder, respectively. I_{yy} represents the mass moment of inertia of vehicle body about y-axis. d_1 and d_2 represent the distance between the CG and the upper springs force and the lower springs force for each vehicle due to pitching rotation, respectively.

There are different types of forces which are applied on the vehicle body. These forces are generated by crushing the front-end structure, conventional suspension system due to the movement of the vehicle body and the active control systems such as the ABS and ASC. The detailed equations of these forces and the validation of the vehicle dynamics–crash model was established in a previous study by the authors (16).

Multi-Body Occupant Model - The occupant mathematical model shown in Figure 2 is developed to evaluate the occupant kinematic behavior in full frontal crash scenarios. The human body model consists of three bodies, with masses m_1, m_2 and m_3. The first body (lower body), with mass m_1, represents the legs and the pelvic area of the occupant and is considered to have a translation motion in the longitudinal direction and rotation motion around the CG of the vehicle. The second body (middle body), with mass m_2, represents the occupant's abdominal area, the thorax area and the arms and is considered to have a translation motion in the longitudinal direction and rotation motion around the pivot between the lower and middle bodies (pivot 1). The third body (upper body), with mass m_3, represents the head and neck of the occupant and is considered to have a translation motion in the longitudinal direction and rotation motion around the pivot between the middle and upper bodies (pivot 2). One rotational spring is considered at each pivot to represent the joint stiffness between the pelvic area and the abdominal area and between the thorax area and the neck/head area, respectively. The seatbelt is represented by two linear spring-damper units between the compartment and the occupant; and the airbag is represented by one linear spring-damper unit.

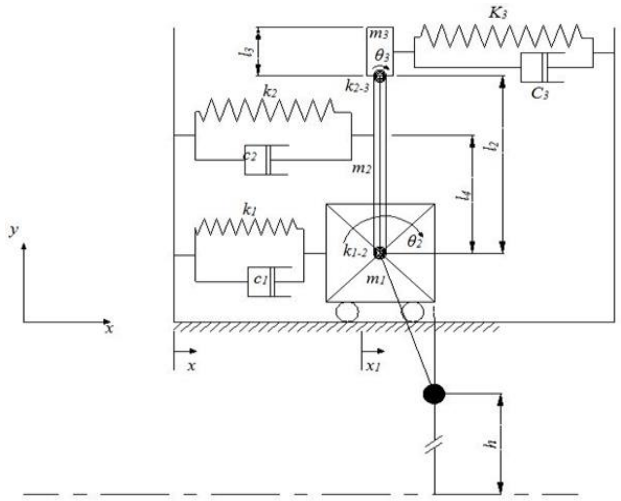

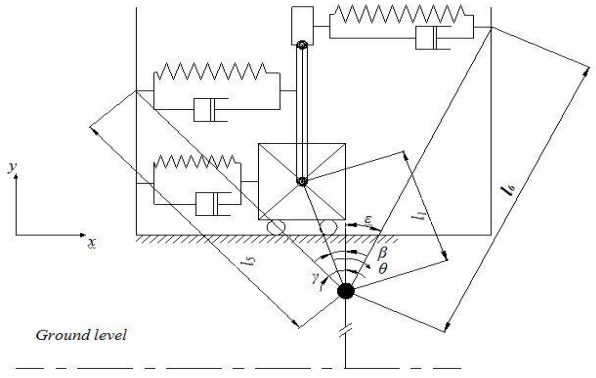

FIGURE 2. MULTI-BODY OCCUPANT MODEL

The equation of motion of the human body, using Lagrange's method, is generated as following:

$$\frac{d}{dt}\left(\frac{\partial E}{\partial \dot{x}_1}\right) - \frac{\partial E}{\partial x_1} + \frac{\partial V}{\partial x_1} + \frac{\partial D}{\partial \dot{x}_1} = 0 \quad (9)$$

$$\frac{d}{dt}\left(\frac{\partial E}{\partial \dot{\theta}_2}\right)-\frac{\partial E}{\partial \theta_2}+\frac{\partial V}{\partial \theta_2}+\frac{\partial D}{\partial \dot{\theta}_2}=0 \quad (10)$$

$$\frac{d}{dt}\left(\frac{\partial E}{\partial \dot{\theta}_3}\right)-\frac{\partial E}{\partial \theta_3}+\frac{\partial V}{\partial \theta_3}+\frac{\partial D}{\partial \dot{\theta}_3}=0 \quad (11)$$

where E, V and D are the kinetic energy, potential energy and the Rayleigh dissipation function of the system, respectively. x_1, θ_2 and θ_3 are the longitudinal movement of the occupant's lower body, the rotational angle of the occupant's middle body and the rotational angle of the occupant's upper body, respectively and $\dot{x}_1$, $\dot{\theta}_2$ and $\dot{\theta}_3$ are their velocities, respectively.

The kinetic energy of the system can be written as:

$$E=\frac{m_1\cdot v_1^2}{2}+\frac{m_2\cdot v_2^2}{2}+\frac{m_3\cdot v_3^2}{2}+\frac{I_1}{2}\cdot\dot{\theta}^2+\frac{I_2}{2}\cdot\dot{\theta}_2^2+\frac{I_3}{2}\cdot\dot{\theta}_3^2 \quad (12)$$

where v_1, v_2 and v_3 are the equivalent velocities of the lower, middle and upper bodies of the occupant, respectively. I_1, I_2 and I_3 are the rotational moment of inertia of the lower, middle and upper bodies about the CG of each body, respectively. The equivalent velocities of the three bodies of the occupant can be calculated as follows:

$$v_1^2=\dot{X}_{m_1}^2+\dot{Y}_{m_1}^2 \quad (13.a)$$

where the displacement and velocity of the lower body in x direction can be calculated as:

$$X_{m_1}=x_1+l_{1o}\cdot(\sin\beta-\sin(\beta-\theta)) \quad (13.b)$$

$$l_1=\sqrt{[l_{1o}\sin(\beta-\theta)-x_1]^2+[l_{1o}\cos(\beta-\theta)]^2} \quad (13.c)$$

based on the small change in θ during the crash event, l_1 has been taken as constant in all equations.

$$\dot{X}_{m_1}=\dot{x}_1+l_1\cdot\dot{\theta}\cdot\cos(\beta-\theta) \quad (13.d)$$

and the displacement and velocity of the lower in y direction can be calculated as:

$$Y_{m_1}=l_1\cdot(\cos(\beta-\theta)-\cos\beta) \quad (13.e)$$

$$\dot{Y}_{m_1}=l_1\cdot\dot{\theta}\cdot\sin(\beta-\theta) \quad (13.f)$$

substituting equations 13.d and 13.f in equation 13.a, the equivalent velocity of the lower body can be determined. By repeating the previous steps of these equations (from equation 13.a to equation 13.f), the equivalent velocities of the middle and upper bodies can be calculated.

where X_{mi} is the resultant longitudinal displacement and Y_{mi} is the resultant vertical displacement. (i: denotes body position 1: lower, 2: middle and 3: upper), l_1, l_2 and l_3 are the distance from the vehicle's CG to the lower body's CG, middle body length and upper body length, respectively. It is assumed that l_1 is constant due to the insignificant change of its length during the crash. β is the angle between the vertical centerline of the vehicle and the line between the vehicle's CG and the CG of the lower body, see Figure 3.

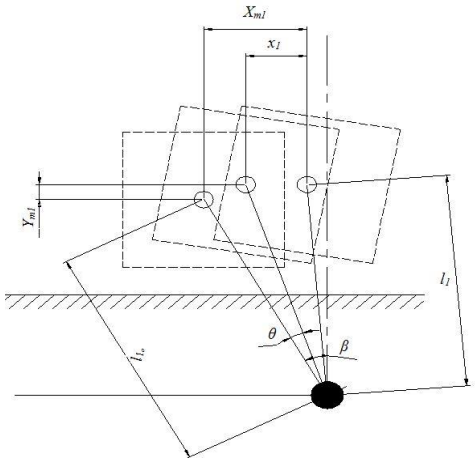

FIGURE 3. A SCHEMATIC DIAGRAM OF THE OCCUPANT'S LOWER BODY MOVEMENT DURING THE IMPACT

By substituting the equivalent velocities of the three bodies in equation 12, the kinetic energy can be obtained.

The potential energy of the system can be written as:

$$V=m_1\cdot g\cdot(h+z+Y_{m_1})+m_2\cdot g\cdot(h+z+Y_{m_1}+\frac{l_2}{2}\cdot\cos\theta_2)$$
$$+m_3\cdot g\cdot(h+z+Y_{m_1}+l_2\cdot\cos\theta_2+\frac{l_3}{2}\cdot\cos\theta_3)+\frac{k_1}{2}\cdot(\delta_1-\delta_{s1})^2$$
$$+\frac{k_2}{2}\cdot(\delta_2-\delta_{s2})^2+\frac{k_3}{2}\cdot(\delta_3-\delta_{s3})^2+\frac{k_{R12}}{2}\cdot(\theta_2-\theta)^2+\frac{k_{R23}}{2}\cdot(\theta_3-\theta_2)^2 \quad (14)$$

where h is the vehicle's CG height. k_1, k_2, k_{R12} and k_{R23} are the lower seatbelt stiffness, upper seatbelt stiffness, the spring stiffness of the pivot 1, and the spring stiffness of the pivot 2, respectively. δ_1, δ_2, δ_3, δ_{s1} δ_{s2} and δ_{s3} are the total deflection of the lower seatbelt spring, total deflection of the upper seatbelt spring, total deflection of the airbag, the initial slack length of the lower seatbelt spring, the initial slack length of the upper seatbelt spring, and the initial slack length of the airbag, respectively. l_4 is the distance between the pivot 1 and the contact point between the upper seatbelt spring and the middle body, l_5 is the distance between the vehicle's CG and the contact point between the upper seatbelt spring and the vehicle compartment, l_6 is the distance between the vehicle's CG and the steering wheel.

The Rayleigh dissipation function can be written as:

$$D=\frac{c_1}{2}\cdot(\dot{x}_1-\dot{x})^2+\frac{c_2}{2}\cdot(\dot{x}_1-\dot{x}+l_4\cdot\dot{\theta}_2\cdot\cos\theta_2-l_5\cdot\dot{\theta}\cdot\cos(\gamma-\theta))^2$$
$$+\frac{c_3}{2}\cdot(\dot{x}_1-\dot{x}+l_2\cdot\dot{\theta}_2\cdot\cos\theta_2+\frac{l_3}{2}\cdot\dot{\theta}_3\cdot\cos\theta_3-l_6\cdot\dot{\theta}\cdot\cos(\varepsilon+\theta))^2 \quad (15)$$

where c_1, c_2 and c_3 are the damping ratio of the lower seatbelt damper, the damping ratio of the upper seatbelt damper, and the damping ratio of the airbag damper, respectively.

To get the components of the equations 9, 10 and 11 the differentiations of the kinetic energy, potential energy, and Rayleigh dissipation function are determined. After that, different occupant's bodies responses (x_1, θ_2 and θ_3) can be determined by solving the equations.

NUMERICAL SIMULATION

In this section, the analysis developed in the former sections is verified by the presentation of the simulation results. Two sets of analysis are carried out in this section. The first set includes a full frontal impact between vehicle "**b**" (standard vehicle in a free rolling scenario) and vehicle "**a**" (equipped with the extendable bumper and VDCS). The VDCS in the case includes anti-lock braking system (ABS) integrated with under-pitch control (UPC) technique. The UPC is developed with the aid of the ASC system using the fuzzy logic controller. The idea of the UPC controller technique is to give the vehicle body negative pitch angle before the crash and try to maintain the vehicle in this case until it collides with the other vehicle. The objective of the UPC system is to obtain the minimum pitching angle and acceleration of the vehicle body during the crash.

The second set of analysis also includes a full frontal impact between vehicle "**b**" (standard vehicle in a free rolling scenario) and vehicle "**a**" (equipped only with VDCS). The VDCS in the case includes anti-lock braking system (ABS) integrated with under-pitch control (UPC). The extendable bumper won't be used in this case to clarify the VDCS effects on the collision mitigation.

Primary Impact Results - While the ADAS detected that the crash is unavoidable at 1.5 sec prior to the impact (17), the VDCS and the extendable bumper will be activated in this short time prior the impact. The values of different parameters used in numerical simulations are given in Table 1 (18); while the damping coefficient and the length of the hydraulic cylinder of the extendable bumper system are chosen to be 20000 N.s/m, and 0.4 m, respectively. The vehicles are adapted to collide with each other with the same velocity of 55 km/hr. Prior collisions, the front-springs forces are equal to zero in the equations of motion. The front-end spring's forces are re-deactivated at the end of collision (vehicle's velocity equal zero/negative values) and the behavior of the vehicle in post-collision is captured.

Parameter	m	I_{yy}	k_{Sf}	k_{SrR}	$c_{fR}=c_{fL}$	$c_{rR}=c_{rL}$	l_f	l_r
Value	1200 kg	1490 kg.m^2	36.5 kN/m	27.5 kN/m	1100 N.s/m	900 N.s/m	1.185 m	1.58 m

TABLE 1: VALUES OF DIFFERENT PARAMETERS USED IN SIMULATIONS FOR BOTH VEHICLES (19).

The following results compare the dynamic response and crash response of the two vehicles involved in a full frontal collision for both sets of analysis defined early. Figure 4 shows the front-end structure's deformation-time histories for both vehicles. It is noticed that when the extendable bumper is not used, the deformation increased to reach its maximum value and then decreased slightly due to front-end springs rebound. A reduction of about 20 mm of the maximum deformation is obtained in vehicle "**a**" compared with vehicle "**b**". When the extendable bumper is applied to vehicle "**a"**, the deformation of the front- end increased slowly to reach a specific point (at around 0.05 sec); at this point the extendable bumper is completely deformed. Then the deformation increased rapidly to reach its maximum value and then decreased slightly due to the rebound effect.

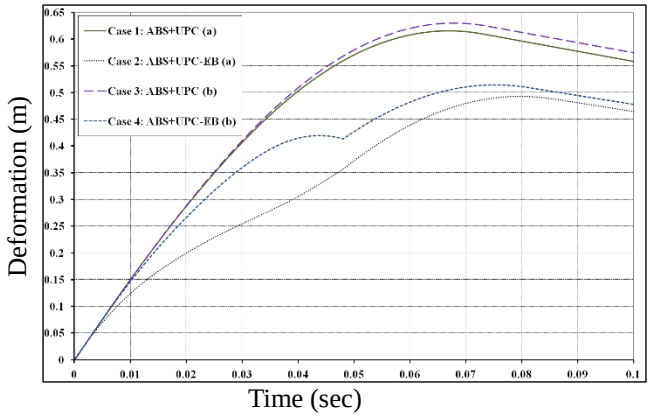

FIGURE 4: DEFORMATION OF THE FRONT-END STRUCTURE

The fundamental advantage of the extendable bumper is to absorb more crash energy by the ability of use more distance available for crush. Therefore, the significant reduction in the front-end deformation shown in Figure 4 is logic. The effect of UPC system helps also reducing the deformation of vehicle "**a**", and it becomes more efficient when the extendable bumper is applied. The reduction of the maximum deformation is increased to be about 25 mm compared with vehicle "**b**", which is greater than the reduction obtained without the use of the extendable bumper.

The deceleration-time histories of both vehicles are illustrated in Figure 5. Without using the extendable bumper, the deceleration- time history can be divided to three stages. The first stage represents the increase of the vehicle's deceleration before the front wheels reach the other vehicle. In this stage, a slight higher deceleration is noticed for vehicle "**a**" due to the application of the ABS. In the second stage, the frontal wheels reach the other vehicle and stop moving; therefore their braking effects are vanished. At the beginning of this stage a rapid reduction in the vehicle "**a**" deceleration occurs (arrow 1, Figure 5). This drop does not appear for vehicle "**b**" because it is collided at a free rolling condition, no braking effect. At the end of this stage, the vehicle stops and starts moving in the opposite direction. In addition, the braking force changes its direction and another drop in the vehicle deceleration is noticed as also shown in Figure 5, (arrow 2). The maximum deceleration is observed in this stage and it is almost the same for both vehicles. At the third stage, a condition of allowing the front- end structure to be rebounded for a very short time is applied during the simulation analysis. During this stage, the vehicle moves back and the deformation of the front-end decreases as shown in Figure 4. At the end of this stage, the non-linear front-end springs are deactivated and the vehicle's deceleration is suddenly dropped to a value of zero. This fast drop is due to the assumption of immediate

stopping the effect front-end springs after very short time of rebound.

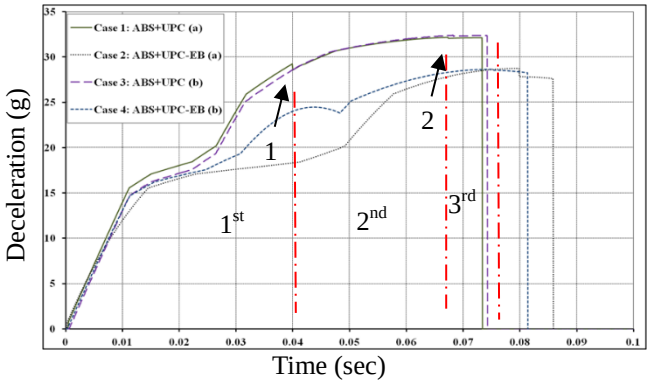

FIGURE 5: VEHICLE BODY DECELERATION

When vehicle "**a**" is equipped with the extendable bumper, the front wheels do not reach the other vehicle; therefore, the second stage does not exist when the extendable bumper is applied. Since the point of impact until the extendable bumper is completely compressed (between 0.04 and 0.05 sec), a higher deceleration is noticed for vehicle "**b**" compared with vehicle "a". After this point, a rapid increase of the deceleration for both vehicles is noticed. The maximum deceleration is almost the same for both vehicles; however, the average deceleration of vehicle "**a**" is less than vehicle "**b**". It is clear from Figure 5 that the maximum deceleration for the two vehicles are low (28 g) when the extendable bumper is used compared with (32 g) when the extendable bumper is not applied. It is also obvious that the effect of the UPC system on vehicle deceleration is insignificant.

Figure 6 shows the vehicle's pitch angle-time histories for both vehicles. The UPC system is applied 1.5 second before collision, therefore, the vehicle body impacts the other vehicle at different value of pitch angles as shown in Figure 6. The vehicle's pitch angle then reaches its maximum values (normally after the end of crash) according to the crash scenario. Following this, the pitch angle reduced to reach negative values and then bounces to reach its steady-state condition.

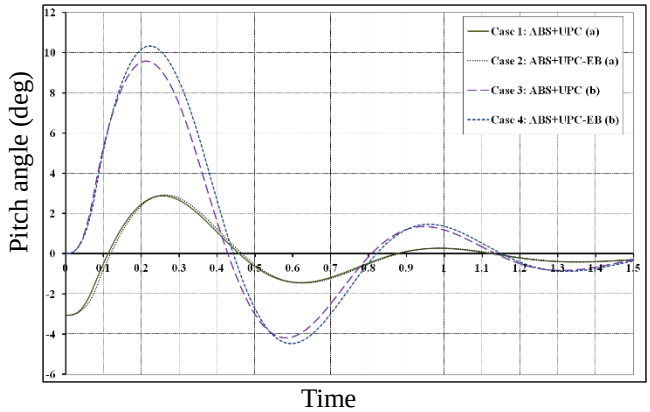

FIGURE 6: VEHICLE BODY PITCH ANGLE

When the under pitch technique is applied along with ABS, the vehicle is given a negative pitch angle prior to impact, and the UPC forces generate a negative pitch moment prior and during the impact. In this case a great improvement of the vehicle pitching is obtained for vehicle "**a**". It is noticed that the use of the extendable bumper does not affect the pitching angle of vehicle "**a**", however, it affects vehicle "**b**" negatively. The pitching angle of vehicle "**b**" is increased by a value equal to about 0.7 deg, and this small value in fact is insignificant.

The vehicle pitch acceleration-time histories are depicted in Figure 7 for both vehicles. The pitch acceleration is increased very quickly at the early stage of the impact to reach its maximum value for each crash scenario due to the high pitching moment generated from the collision. At the end of the collision, all pitching moments due to the crash are equals to zero, vehicles speeds are negative with very low values, and the vehicle pitch angles are still positive. This means the vehicle is now controlled by the tyres and suspension forces, which have already generated moments in the opposite direction of the vehicle pitching. This describes the reason for the high drop and the changing direction from positive to negative on the vehicle pitch acceleration at the end of the crash.

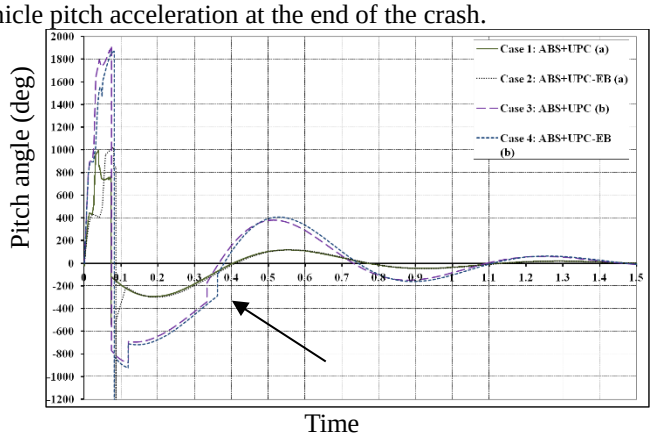

FIGURE 7: VEHICLE BODY PITCH ACCELERATION

As shown in Figure 7, the vehicle's maximum pitching acceleration occurs at the end of the collision. The reduction of the vehicle pitch acceleration in this case is also notable; it decreases from about 1900 deg/s2 in vehicle "**b**" to about 1000 deg/s2 in vehicle "**a**". While the effect of the extendable bumper is insignificant for the maximum pitch acceleration, the mean acceleration, especially for vehicle "**a**", is reduced. The reason of this is that the pitching moment generated from the deformation of the front-end structure is low during the use of the extendable bumper. For vehicle "**b**", because of the vehicle's rear wheels left the ground during the vehicle pitching, a sudden increase of the vehicle pitching acceleration is observed when the rear wheels re-contacted the ground (look at the arrow in Figure 7). This sudden increase in pitching acceleration does not exist in vehicle "**a**" because the rear wheels do not leave the ground due to the reverse pitching moment generated from the UPC system.

Secondary Impact Results - The injury criteria in this paper have been taken as occupant's pelvis deceleration, occupant's chest rotational acceleration, and head rotational acceleration. These injury criteria of the occupant have been determined based on the output data obtained from the vehicle dynamics/crash model. The vehicle output data (deceleration and pitching acceleration) due to the collision are transferred to the occupant as a sudden deceleration to all the body, and rotational movements of the head and chest. It is assumed that at initial condition, the occupant's chest and head are in a vertical position. When the VDCS is applied (1.5 Sec prior collision) the occupant's chest and head will take a different angles in this short time according to each case and then collide with the other vehicle with these different angles. It is also important to mention that the front airbag is activated at the point of impact.

The occupant data that used in the numerical simulation is presented in table 2 (20), while the total stiffness of the two seatbelt springs is 98.1 kN/m with a damping coefficient of 20% (8), and then it distributed between the upper and lower seatbelt springs by a ratio of 2:3, respectively (21). Airbag's spring stiffness is 5 kN/m and the damping coefficient is 20%. The slacks of the seatbelt springs are assumed zero, and the slack of the airbag is 0.05 m.

Parameter	m_1	m_2	m_3	k_{R12}	k_{R23}	L_2	L_3
Value	26.68 kg	46.06 kg	5.52 kg	280 Nm/rad	200 Nm/rad	0.427 m	0.24 m

TABLE 2: THE VALUES OF THE OCCUPANT PARAMETERS

The longitudinal displacement of the pelvis is depicted for all cases in Figure 8; it increases forward to reach its maximum position almost at the end of impact, and then returns back due to the seatbelt springs effect. The fundamental advantage of the extendable bumper is to absorb more crash energy with the ability to use more distance available for crush. Therefore, the significant reduction in the pelvis' longitudinal displacement shown in Figure 8 is a logic. It is noticed that for the first set of results (without the extendable bumper) slight differences in the maximum displacement of the occupant's pelvis.

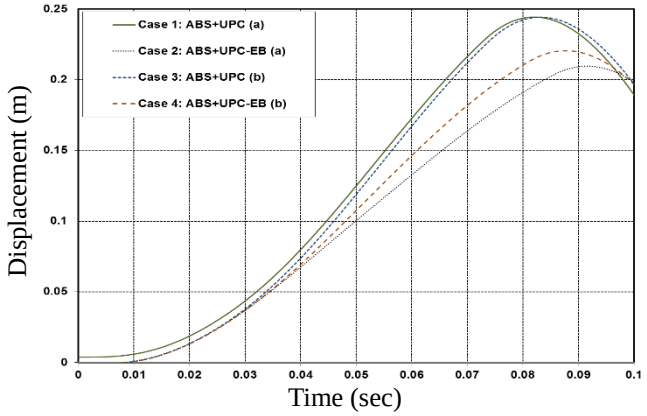

FIGURE 8: OCCUPANT'S PELVIS DISPLACEMENT FOR ALL CASES

For the second set of results (with the extendable bumper), the pelvis' displacement increased slowly compared with the first set of results to reach its maximum value and then decreased slightly due to the seatbelt rebound. It is observed from Figure 8 that there is a significant reduction in the values of the maximum displacement of the occupant's pelvis. It is also noticed that the UPC system helps for more reductions of vehicle (a).

Figure 9 shows the pelvis deceleration for all cases; it is shown that it increases during the collision to reach its maximum values at the end of impact and then reduces due to the seat belt effect. The sudden decrease of the deceleration (arrow 1 in the figure) is due to the reverse of the effect of the braking force at the end of impact when the vehicle changes its direction and starts to move backward. It observed that the maximum deceleration is almost the same in the case of only UPC is applied. When the extendable bumper is used the deceleration of the pelvis relative deceleration is noteworthy reduced with a higher (insignificant) values with UPC.

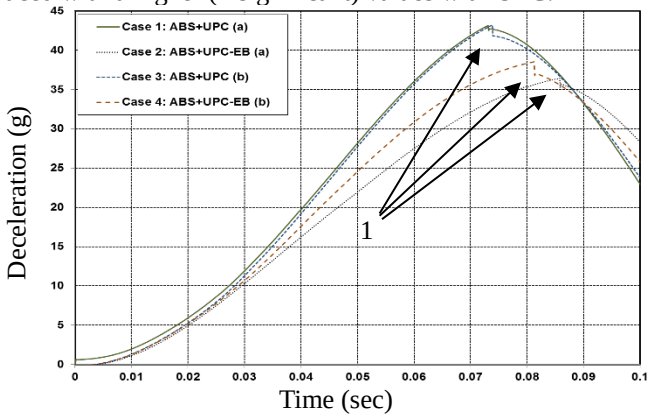

FIGURE 9: OCCUPANT'S PELVIS DECELERATION FOR ALL CASES

The relative rotation angle and acceleration of the occupant's chest for all cases are shown in Figures 10 and 11, respectively. The occupant's chest starts the collision with different rotational angles according to each case. The occupant takes this angle in the period of 1.5 Sec prior collision when the VDCS is applied. The chest rotational angle is increased to reach its maximum value after about 0.06 second from the end of impact. It is observed that the UPC system plays a significant role to reduce the rotation angle of the occupant's chest when it is applied on vehicle (a). On the other hand the extendable bumper helps to reduce this rotational angles for both vehicles. The reduction of about 10 degrees is obtained for vehicle (a) compared with vehicle (b) due to application of UPC and extra 5 degrees are reduced because of the extendable bumper. Related to the rotational acceleration, the positive rotational acceleration shown in Figure 11 is due to the vehicle crash, while the negative maximum acceleration is due to the return of the seatbelt springs effect. The chest rotational

acceleration increases gradually to reach its maximum positive value and then reduces to reach its maximum negative value. For both sets of results, it is monitored that the minimum positive acceleration is occurred when the UPC is applied with the extendable bumper for vehicle (a), while the minimum one in the negative acceleration is happening in vehicle (b). The effect of the control system and the extendable bumper is appear only on the positive acceleration.

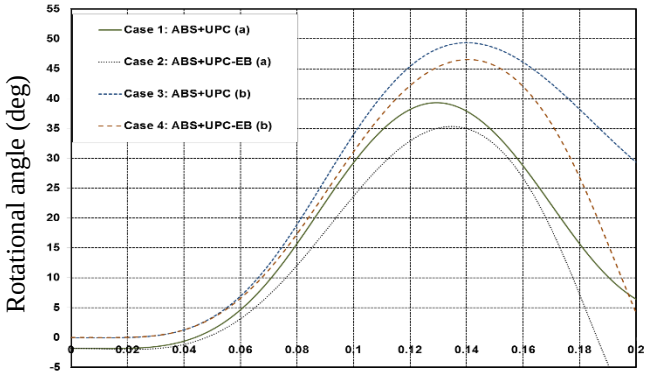

FIGURE 10: ROTATIONAL ANGLE OF THE OCCUPANT'S CHEST ABOUT Y AXIS FOR ALL CASES

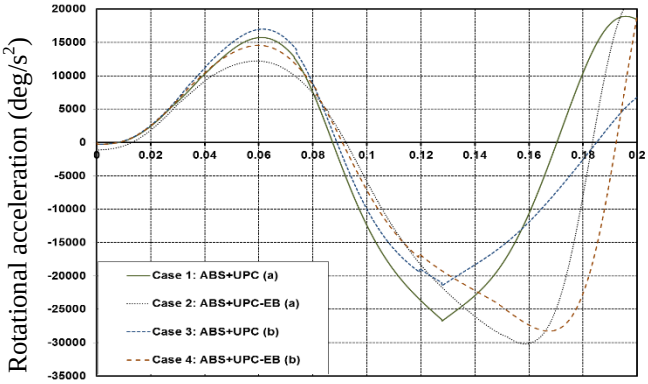

FIGURE 11: ROTATIONAL ACCELERATION OF THE OCCUPANT'S CHEST FOR ALL CASES

The relative rotation angle between the occupant's chest and head is captured in Figures 12. The head rotation angle is increased to reach its first peak values, which is occurring during the increase of chest rotating. Then it increased gradually to reach its second peak values, except in case 2, due to the return of the occupant's chest. It is clear that the UPC help reducing the rotation of the occupant's head in vehicle (a), for about 20 degrees compared with vehicle (b), which is not occupied by VDCS. The application of the extendable bumper has a great effect on reducing the maximum rotation angles of the occupant's head for both vehicles especially for the second peak (which is eliminated in vehicle (a)) as shown in Figure 12. Figure 13 shows the relative rotational acceleration of the occupant's head. The maximum positive and negative acceleration are observed for vehicle (b) in the case UPC is only applied (without the extendable bumper), while the minimum positive and negative values are seen for vehicle (a) when the UPC is applied with the extendable bumper.

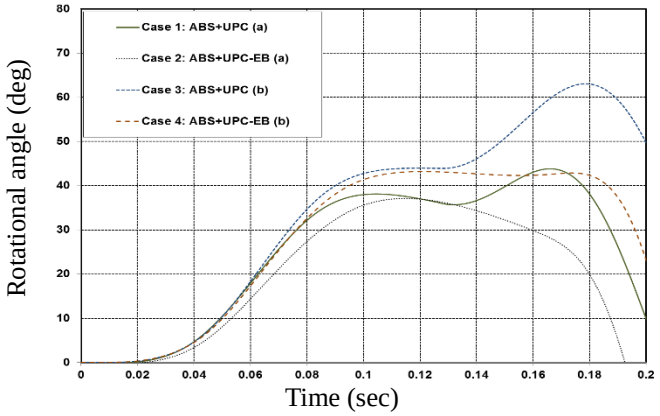

FIGURE 12: ROTATIONAL ANGLE OF THE OCCUPANT'S HEAD FOR ALL CASES

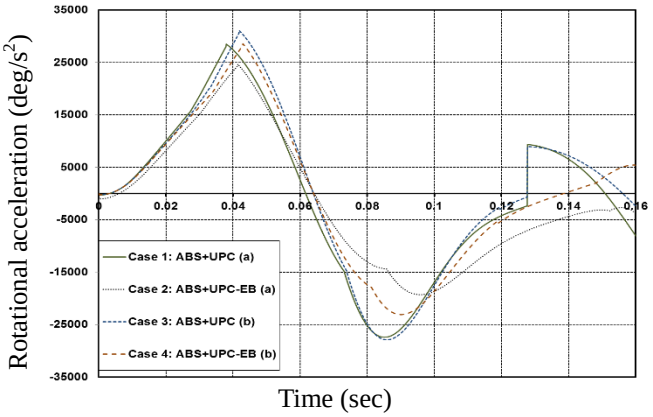

FIGURE 13: ROTATIONAL ACCELERATION OF THE OCCUPANT'S HEAD FOR ALL CASES

Related to the occupant injury criteria, the occupant's head rotational accelerations appeared to be the major cause of strain-induced brain injury which it contributed to more than 80% of the brain strain and the peak amplitude of rotational acceleration must not exceed 9.4 krad/s2 (538.5 kdeg/s2) (22). The results show some improvement in the occupant injury criteria, which makes the crash event more survivable. Use of under pitch technique along with the extendable bumper can help reduce the chest and head rotation angle, and head rotational acceleration.

CONCLUSION

A unique vehicle dynamics/crash mathematical model is developed to study the influences of VDCS integrated with the extendable bumper system on the vehicle collision mitigation. This model combines vehicle crash structures, vehicle dynamics control and extendable bumper systems. In addition, a multi-body occupant mathematical model has been developed to capture the occupant dynamic response. It is shown from

numerical simulations that the extendable bumper surpasses the traditional structure in absorbing crash energy at the same crash speed. Furthermore, it is shown that the extendable bumper brings significantly lower intrusions and helps keep the vehicle deceleration within desired limits. The results obtained from different applied cases show that the VDCS affect the crash situation positively. The deformation of the vehicle front-end structure is reduced when the VDCS is applied, and this reduction in the vehicle deformation is greater when the extendable bumper is used. The vehicle body deceleration is insignificantly changed within the applied of VDCS. The vehicle pitch angle and its acceleration are dramatically reduced when the ABS is applied alongside the UPC system. It is also shown that the extendable bumper beats the traditional structure in occupant injury criteria. On the other hand, there are a significant effect of the VDCS on the rotations angle and acceleration of the occupant chest and head.

ACKNOWLEDGMENT

The authors would like to thank the Egyptian Government and the Faculty of Engineering, Ain Shams University for supporting this research. The authors also acknowledge with sadness, the contribution of Prof. Dave Crolla who has passed away during the period of this research.

REFERENCES

1. Hobbes C (1991) The Need for Improved Structural Integrity in Frontal Car Impacts. 13th ESV Conference, Paris, France: 1073-1079.
2. Mizuno K, Umeda T, Yonezawa H (1997) The Relation between Car Size and Occupant Injury in Traffic Accidents in Japan.
3. Hiroyuki M (1990) A Parametric Evaluation of Vehicle Crash Performance.
4. Elsholz J (1974) Relationship between Vehicle Front-End Deformation and Efficiency of Safety Belts during Frontal Impact. 5th ESV Conference, London, England: 674-681.
5. Tamura M, Inoue H, Watanabe T, Maruko N (2001) Research on a Brake Assist System with a Preview Function.
6. Sugimoto Y, Sauer C (2005) Effectiveness Estimation Method for Advanced Driver Assistance System and its Application to Collision Mitigation Brake System.
7. Elmarakbi A, Zu J (2004) Dynamic Modelling and Analysis of Smart Vehicle Structures for Frontal Collision Improvement. International Journal of Automotive Technology 5: 247-255.
8. Elmarakbi A, Zu J (2005) Crashworthiness Improvement of Vehicle-to-Rigid Fixed Barrier in Full Frontal Impact using Novel Vehicle's Front-End Structures. International Journal of Automotive Technology 6: 491-499.
9. Yu F, Feng JZ, Li J (2002) A Fuzzy Logic Controller Design for Vehicle Abs with a On-Line Optimized Target Wheel Slip Ratio. International Journal of Automotive Technology 3: 165–170.
10. Yue C, Butsuen T, Hedrick J (1988) Alternative Control Laws for Automotive Active Suspensions. American Control Conference, USA: 2373 –2378.
11. Alleyne A, Hedrick JK (1995) Nonlinear Adaptive Control of Active Suspensions. IEEE Transactions on Control Systems Technology 3: 94 –101.
12. Mastandrea M, Vangi D (2005) Influence of Braking Force in Low-Speed Vehicle Collisions. Journal of Automobile Engineering 219: 151–164.
13. Hogan I, Manning W (2007) The Use of Vehicle Dynamic Control Systems for Automotive Collision Mitigation. 3rd Institution of Engineering and Technology Conference on Automotive Electronics, USA: 1 -10.
14. Kamal M (1970) Analysis and Simulation of Vehicle to Barrier Impact. SAE International, Warrendale, PA, Technical Paper 700414.
15. Khattab A (2010) Steering System and Method for Independent Steering of Wheels (Ph.D. Thesis), The department of Mechanical and Industrial Engineering, Concordia University Montreal, Quebec, Canada.
16. Elkady, M, Elmarakbi, A (2012) Modelling and Analysis of Vehicle Crash System Integrated with Different VDCS under High Speed Impacts. Central European Journal of Engineering, Vol. 2, No. 4, pp.585-602.
17. Jansson J, Gustafsson F, Jonas J (2002) Decision Making For Collision Avoidance Systems.
18. Alleyne A (1997) Improved Vehicle Performance using Combined Suspension and Braking Forces. Vehicle System Dynamics 27: 235–265.
19. Alleyne, A (1997) Improved Vehicle Performance Using Combined Suspension and Braking Forces. Vehicle System Dynamics, 27, 4, 235–265.
20. Ilie, S., Tabacu, S (2007) Study of the occupant's kinematics during the frontal impact. Annals of the Oradea University, Fascicle of Management and Technological Engineering, VI (XVI).
21. Paulitz, T J, Blackketter, D M, Rink, K K (2006). Constant force restraints for frontal collisions. Proceedings of the Institution of Mechanical Engineering, Part D: Journal of Automobile Engineering, 220(9), pp. 1177-1189
22. Zhang, J, Pintar, F (2006). Brain Strains in Vehicle Impact Tests. Annual Proceedings Associated Advanced Automotive Medicine, 50, pp. 1-12.

.